Evaluating spatial and temporal patterns of MODIS GPP over the conterminous U.S. against flux measurements and a process model

Fangmin Zhang [a,b,*], Jing M. Chen [b], Jiquan Chen [c], Christopher M. Gough [d], Timothy A. Martin [e], Danilo Dragoni [f]

[a] *Jiangsu Key laboratory of Agricultural Meteorology, College of Applied Meteorology, Nanjing University of Information Science and Technology, Nanjing, 210044, China*
[b] *Department of Geography and Program in Planning, University of Toronto, Toronto, Canada M5S 3G3*
[c] *Department of Environmental Sciences, University of Toledo, Toledo, OH 43606-3390, USA*
[d] *Virginia Commonwealth University, Richmond, VA 23284-2012, USA*
[e] *School of Forest Resources and Conservation, University of Florida, Gainesville, FL 32611-0410, USA*
[f] *Department of Geography, Indiana University, Bloomington, IN 47405, USA*

ARTICLE INFO

ABSTRACT

Gross primary productivity (GPP) quantifies the photosynthetic uptake of carbon by ecosystems and is an important component of the terrestrial carbon cycle. Empirical light use efficiency (LUE) models and process-based Farquhar, von Caemmerer, and Berry (FvCB) photosynthetic models are widely used for GPP estimation. In this paper, the MODIS GPP algorithm using the LUE approach and the Boreal Ecosystem Productivity Simulator (BEPS) based on the FvCB model in which a sunlit and shaded leaf separation scheme is evaluated against GPP values derived from eddy-covariance (EC) measurements in a variety of ecosystems. Although the total GPP values simulated using these two models agree within 89% when they are averaged for the conterminous U.S., there are systematic differences between them in terms of their spatial and temporal distribution patterns. The spatial distribution of MODIS GPP therefore differs substantially from that produced by BEPS. These differences may be due to an inherent problem of the LUE modeling approach. When a constant maximum LUE value is used for a biome type, this simplification cannot properly handle the contribution of shaded leaves to the total canopy-level GPP. When GPP is modeled by BEPS as the sum of sunlit and shaded leaf GPP, the problem is minimized, i.e., at the low end, the relative contribution of shaded leaves to GPP is small and at the high end, the relative contribution of shaded leaves is large. Compared with monthly and annual GPP derived from eddy covariance data at 40 tower sites in North America, BEPS performed better than the MODIS GPP algorithm. The difference between MODIS and BEPS GPP widens as with the fraction of shaded leaves increases. The simpler LUE modeling approach should therefore be further improved to reduce this bias issue for effective estimation of regional and temporal GPP distributions.

© 2012 Elsevier Inc. All rights reserved.

1. Introduction

The terrestrial gross primary productivity (GPP), defined as the total photosynthetic uptake of carbon per unit of time and space, is a critical variable in terrestrial biosphere models (TBM), as it often represents the control factor for many other processes in the model (Jung et al., 2007). However, estimates of GPP can vary greatly among TBM, even under similar environmental conditions, because of different algorithms used to describe the basic photosynthetic processes in response to environmental conditions (Coops et al., 2009). Validation of these algorithms against GPP observations is therefore critical to improve the performances of TBM and our understanding of the interactions between terrestrial ecosystems and the atmosphere.

Different underlying assumptions on the mechanisms and controls of the photosynthetic process, and the spatio-temporal resolution of the associated biotic and abiotic drivers originated a wide variety of TBM. For example, some prognostic TBM estimate GPP based on surface observations, like soil and meteorological conditions (Foley et al., 1996; Haxeltine & Prentice, 1996; Polcher et al., 1998). However, remote sensing observations are particularly useful for assessing the regional distribution of GPP using diagnostic TBM (Ruimy et al., 1999). Despite the large number of TBM available, it is possible to identify two main strategies used to estimate GPP. In the first group of models an empirical relationship is used to quantify GPP as a function of light use efficiency (LUE) and environmental conditions (Houborg et al., 2009). In these models (henceforth, LUE models), such as CASA (Potter et al., 1993), GLO-PEM (Prince & Goward, 1995), and the MODIS algorithm (Zhao & Running, 2010), GPP is proportional to the photosynthetically active radiation (PAR) absorbed by the canopy (APAR), and LUE is derived from empirical observations of GPP and APAR (Montieth, 1972). One advantage of LUE

models is the very limited number of parameters required to characterize LUE under non-water limited conditions and for specific vegetation types. However, the reliability of this approach in assessing GPP, in particular for spatial and temporal scales beyond those used to derive the empirical relationships, has been questioned, and modifications of the original approach have been proposed (Sims et al., 2008).

The second group of TBM is based on the mechanistic description of the photosynthetic biochemical processes occurring at leaf level (Farquhar et al., 1980). In these models (henceforth, process-based models), such as SIB2 (Sellers et al., 1996), BIOME3, CLASS (Wang et al., 2001), Boreal Ecosystem Productivity Simulator (BEPS) (Chen et al., 1999), and InTEC (Chen et al., 2000), GPP is first computed at the leaf level and then scaled-up to the whole canopy Big-leaf models, which reduce the complexity of the canopy to a single leaf (Sellers et al., 1996) have been extensively used mainly for their simplicity, but have been shown to introduce significant errors into the calculations of canopy photosynthesis (Dai et al., 2004; De Pury & Farquhar, 1997; Norman, 1980; Wang & Leuning, 1998). Another scaled-up approach is to separate a canopy into multiple layers and to integrate them for the whole canopy to obtain the canopy-level flux (Leuning et al., 1995). The multiple-layer approach overcomes the limitation of the big-leaf approach, but is itself limited by the ability to reliably describe the structural and functional complexity of the canopy. The two-leaf approach differentiates between sunlit and shaded leaves and largely overcomes the deficiencies of the big-leaf approach, as it includes the highly non-linear response of leaf photosynthesis under sunlit and shaded conditions (Norman, 1982). In addition, this approach does not require the same level of complexity in describing the canopy structure and it is computationally more efficient than the multi-layer scheme (Dai et al., 2004; Wang & Leuning, 1998).

LUE- and process-based models differ in their ways of simulating photosynthesis processes and overall complexities. We therefore expect differences in the simulated GPP between these two approaches. The objectives of this study are to (1) quantify the biases existing with LUE models in generating the spatial and temporal distribution patterns of GPP and (2) investigate the underlying reasons for these biases using a process-based model. The BEPS model, which is a process-based two-leaf model (Chen et al., 1999; Ju et al., 2006; Liu et al., 1997), is used for this purpose. Monthly and annual GPP values, simulated by the MODIS algorithm and BEPS, are evaluated against GPP derived from eddy-covariance (EC) measurements from a variety of ecosystems across the continental U.S. from 2000 to 2005.

2. The models

2.1. BEPS model

The BEPS model used in this study is an hourly process-based diagnostic model (Chen et al., 1999; Ju et al., 2006) that computes the canopy-level GPP as the sum of sunlit and shaded leaf groups using the FvCB photosynthesis model (Farquhar et al., 1980). BEPS was initially developed for boreal ecosystems as a daily model (Liu et al., 1997), but it has been expanded for temperate and tropical ecosystems (Feng et al., 2007; Matsushita & Tamura, 2002; Zhang et al., 2010) and modified to run on hourly time-scale (Ju et al., 2006). BEPS is driven by remote sensing, meteorological, and soil data with a set of biome-dependent biophysical parameters. In the hourly version of BEPS, stomatal conductance for sunlit and shaded leaves is iteratively calculated using the Ball–Berry equation (Ball, 1988) and scaled using a soil water stress index (Ju et al., 2006). Despite its intense computational requirements, the hourly version of BEPS, was preferred and used in this work because the stomatal conductance calculation is stable and reliable. On the other side, the parameterization scheme based on Jarvis (1976) lacks sufficient empirical data for simulations at the continental scale (Van Wijk et al., 2000). The major characteristics of BEPS

Table 1
Description of the processed BEPS GPP submodel and MODIS GPP algorithm used in this study.

	Model descriptions	BEPS	MODIS GPP algorithm
Time step		Hourly	8-day
Inputs	Satellite data	LAI	
		Clumping index	MODIS fPAR
		Land cover	Land cover
	Climate data	Temperature	Temperature
		Radiation	Radiation
		Relative humidity	VPD
		Precipitation	
		Wind	
	Atmospheric data	CO_2	\
	Soil data	Soil texture	\
GPP calculation			f(fPAR, LUE,T_{min},PAR,VPD)
Processes	Canopy structure	Two leaves	\
	Distinguish sunlit/ shaded leaves?	Yes	No
	Scaling	Yes	No
	Photosynthesis approach	FvCB	\
	Stomatal conductance	Ball–Berry	\
	Evaportansipiration	Penman–Monteith	Penman–Monteith
	Explicit interception losses of precipitation	Yes	No
	Soil water factor	Yes	\
	Coupled photosynthesis and transpiration	Yes	\
	Rate dynamics	First order	\
	Moisture parameter	SWC	\
	Soil layer	5	\

"FvCB" indicates that photosynthesis calculations are based on enzyme kinetics and light absorption following Farquhar et al. (1980). Here, the FvCB model is applied to sunlit and shaded leaves separately (Norman, 1982). "Ball–Berry" indicates a coupled stomatal conductance-photosynthesis model following Ball (1988) using the relative humidity as a scalar. We use an analytical solution of the Ball–Berry equation to determine stomatal conductance (Baldocchi, 1994) in order to improve the computation efficiency for regional and global simulations.

are summarized in Table 1 and the major functions used in BEPS that are directly relevant to this study are given in Appendix A.

2.2. MODIS GPP algorithm

The MODIS GPP algorithm is designed to provide a regular eight-day measure of the growth of the terrestrial vegetation (Zhao et al., 2005). It is calculated daily at 1 km resolution using an empirical LUE model with the following equations:

$$GPP = LUE \times fPAR \times PAR, \quad (1)$$

$$LUE = LUE_{max} \times f(VPD) \times g(T_{min}), \quad (2)$$

$$fPAR = 1 - e^{-k \times LAI}, \quad (3)$$

where LUE_{max} is the maximum light use efficiency, $f(VPD)$ is the scalar of daily vapor pressure deficit (VPD), $g(T_{min})$ is the scalar of daily minimum air temperature (T_{min}) and fPAR is the fraction of the photosynthetically active radiation absorbed by the canopy. Biome physiological parameters are specified based on the MODIS land cover classification system using a biome property look-up table (BPLUT) (Zhao & Running, 2010; Table 1).

3. Data and methods

All inputs and auxiliary data used in this study, including reanalysis meteorological data from the National Center for Environmental Prediction (NCEP), leaf area index (LAI), foliage clumping index, land cover map, soil texture data, and other vegetation parameters, are described in Section 3.4.

3.1. BEPS GPP

In this study, BEPS is driven by the NCEP reanalysis meteorological data, LAI data produced with cloud-free 10-day SPOT-4 VEGETATION data, the Global Land Cover Map 2000 (GLC2000), foliage clumping index, and soil data at 1 km resolution. Monthly and yearly GPP values are aggregated from hourly values from 2000 to 2005.

3.2. MODIS GPP

MODIS is one of the primary global monitoring sensors on NASA Earth Observing System (EOS) satellites and began providing global GPP products (MOD17) in 2000 (Zhao et al., 2005). The MOD17 monthly and annual products from 2000 to 2005 were used in this work (MOD17A, http://ftp.ntsg.umt.edu/.autofs/MODIS/Mirror/MOD17_Science_2010/) and calculated on daily basis using the MODIS GPP algorithm (Zhao & Running, 2010). The daily meteorological data used to drive the MODIS GPP algorithm, including minimum temperature and VPD derived from the reanalysis data from NCEP, were interpolated to 1 km resolution using the distance-weighted method (Zhao et al., 2005). Remote sensing data, including eight-day fPAR and LAI datasets at 1 km resolution, were from Collection 5 (C5) products of the MODIS sensor. The MODIS GPP products have been tested in previous studies (Coops et al., 2009; Heinsch et al., 2006; Nightingale et al., 2007; Sasai et al., 2005; Sims et al., 2006, 2008; Turner et al., 2003, 2005, 2006; Wu et al., 2010; Xiao et al., 2010; Yang et al., 2007; Zhao et al., 2005, 2006).

3.3. Eddy-covariance (EC) data

EC observations provide invaluable opportunities to evaluate LUE and process-based models because the EC technique measures carbon, water, and energy fluxes between ecosystem surface and atmosphere at very high temporal frequency (i.e., hourly or half-hourly, Baldocchi et al., 2001). The EC data used were downloaded directly from the AmeriFlux website (http://ameriflux.ornl.gov). In the Level 4 product, a continuous record of half-hourly GPP was calculated during daylight hours as net ecosystem exchange minus ecosystem respiration. Data gaps of the half-hourly GPP associated with equipment failures or unsuitable micrometeorological conditions were filled using the Marginal Distribution Sampling (MDS) method (Reichstein et al., 2005) and the Artificial Neural Network (ANN) method (Papale & Valentini, 2003). In particular, monthly GPP was first aggregated from half-hourly values was first gap-filled using the ANN gap-filled approach, whereas monthly GPP was aggregated from half-hourly values using the MDS gap-filled approach when gap-filled half-hourly values from the ANN approach were not available. The uncertainties of monthly and annual EC-GPP (shown in Figs. 1–3) are estimated by standard error (SE) according to measurement and gap filling error reported by each site. Sites were discarded from the dataset if less than three monthly GPP values were available in each growing season. This resulted in a final dataset from 40 AmeriFlux sites across the U.S. (Table 2).

3.4. Regional input data

3.4.1. Meteorological data

Meteorological data, including incoming shortwave radiation, air temperature, specific humidity, precipitation, and wind speed, were obtained from NCEP (http://www.esrl.noaa.gov/psd/data). For hourly modeling, temporal interpolations were made to produce hourly values from the six-hour interval dataset. Different interpolation methodologies were used for the different variables. Specific humidity and wind speed were assumed constant across the six-hour NCEP interval. Total precipitation was equally divided across the six-hour interval. Incoming shortwave radiation was calculated for each hour as a function of the solar zenith angle and daily total incoming shortwave radiation from NCEP. Hourly air temperature was determined with six-hour values

and maximum/minimum values in NCEP data. Hourly NCEP data were bi-linearly interpolated spatially into 1 km × 1 km simulation grids.

3.4.2. Land cover

The Global Land Cover Map 2000 (GLC2000; http://www.eogeo.org/GLC2000) used in this study was produced by SPOT-4 VEGETATION data at 1 km resolution. GLC2000 was derived from daily values of surface reflectance and NDVI based on individual methodologies from different countries. The land cover classifications were aggregated to nine types: evergreen broadleaf forest (EBF), deciduous broadleaf forest (DBF), evergreen needleleaf forest (ENF), deciduous needleleaf forest (DNF), mixed forest (MF), crop, grass, shrub, and savanna.

3.4.3. Leaf area index (LAI)

The LAI dataset from 2000 to 2005 was produced with cloud-free, ten-day synthesis VEGETATION images at 1 km resolution. Reflectance in red, near-infrared (NIR), and mid-infrared (MIR) was used to estimate LAI using the algorithm developed by Deng et al. (2006). This algorithm, based on the 4-Scale geometrical optical model (Chen & Leblanc, 1997), makes use not only of the surface reflectance of each pixel but also of the angular information at the time of data acquisition, including solar zenith angle, view zenith angle, and the difference between sun and satellite azimuth angles. In this regard, the variation of reflectance in the different bands with the angles of sun and satellite (i.e., the bidirectional reflectance distribution functions) is considered. For reliable terrestrial applications of the LAI images, the residual cloud and atmospheric effects in the LAI images are detected and removed using a Locally Adjusted Cubic-spline Capping (LACC) method based on the seasonal trajectory of each grid (Chen et al., 2006). In this algorithm, the effective LAI is derived from the canopy gap fraction retrieved using multispectral data. The actual LAI is calculated from effective LAI using the foliage clumping index (described in the next section) obtained from multi-angle remote sensing. This unique approach is compatible with the need of accurate separation of sunlit and shaded leaves, which requires not only the LAI but also clumping index (Eqs. A7a and A7b), and has been evaluated using data from Canada and the U.S. (Pisek & Chen, 2007).

3.4.4. Clumping index

Structured canopies usually cause large variations in reflectance from the hotspot, where the sun and view angles coincide, to the dark spot, where shadows of clumps are maximally observed. The more clumped a canopy is, the more shadow it has, and hence the darker the dark spot is. An improved angular index, named Normalized Difference between Hotspot and Dark spot (NDHD), was proposed for retrieving the clumping index using multiple-angle remote sensing data (Chen et al., 2005; Leblanc et al., 2005). Through geometrical-optical modeling using the 4-Scale model (Chen & Leblanc, 1997), relationships between NDHD and clumping index were established for various plant functional types (Chen et al., 2005; Pisek et al., 2010). Based on these relationships, a global clumping map at 0.5 km resolution was produced using the MODIS Bidirectional Reflectance Distribution Function product (He et al., 2012). This product was used in the LAI algorithm to convert the effective LAI to the actual LAI and for separation of sunlit and shaded leaves.

3.4.5. Soil texture

Soil texture for each 1° × 1° grid obtained from NASA (Webb et al., 1991) was used to estimate hydrological parameters including porosity, field capacity (water potential at 33 kPa), wilting point (water potential at 1500 kPa), saturated hydraulic conductivity, and air entry water potential (Campbell & Norman, 1998). These parameters were used to calculate the water-holding capacity and the soil water scaling parameter, f_w.

3.5. Analytical methods

All statistical analysis was conducted in SPSS14.0 and Microsoft Excel 2007. Coefficients of determination (R^2), slope, root mean
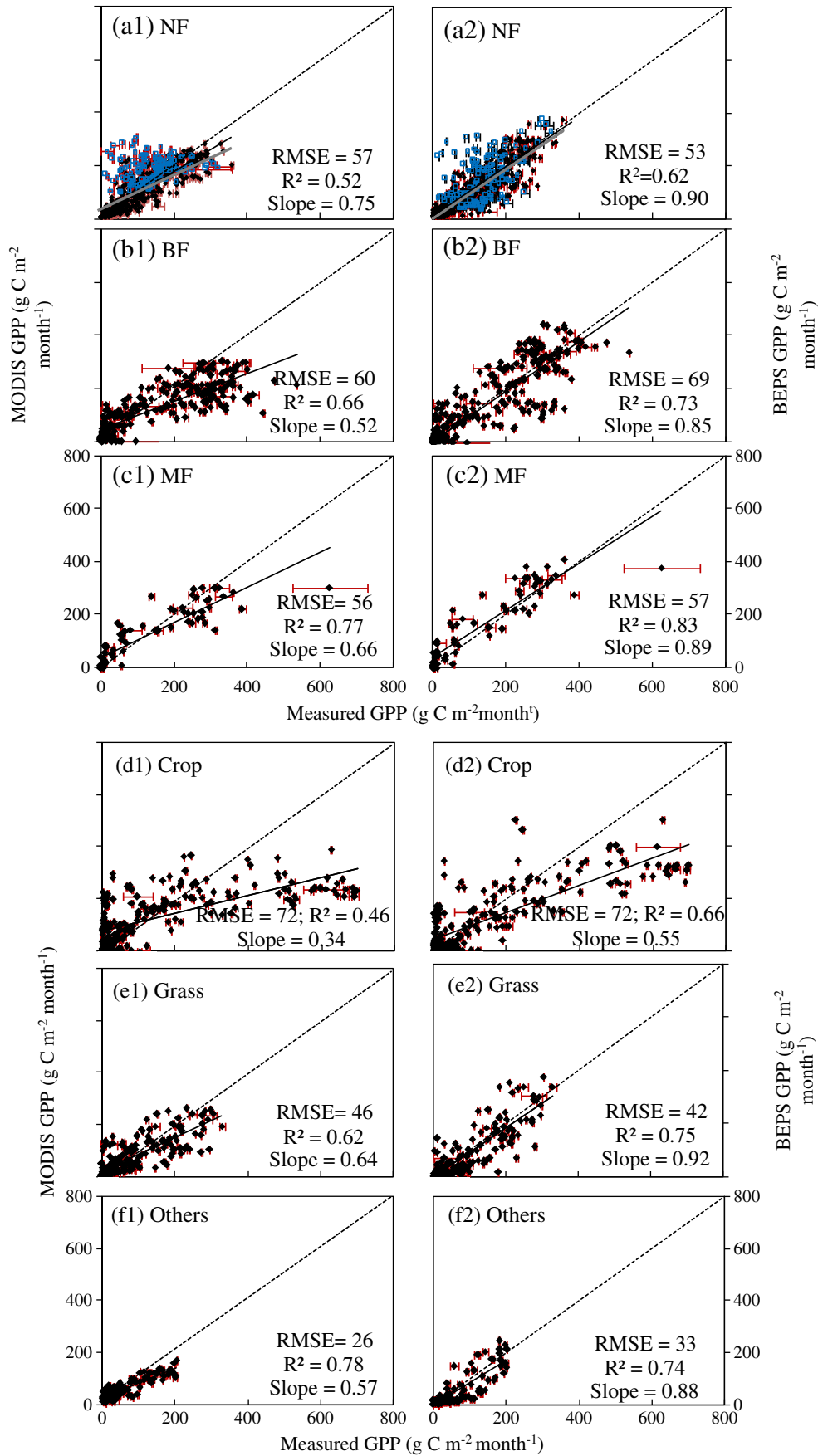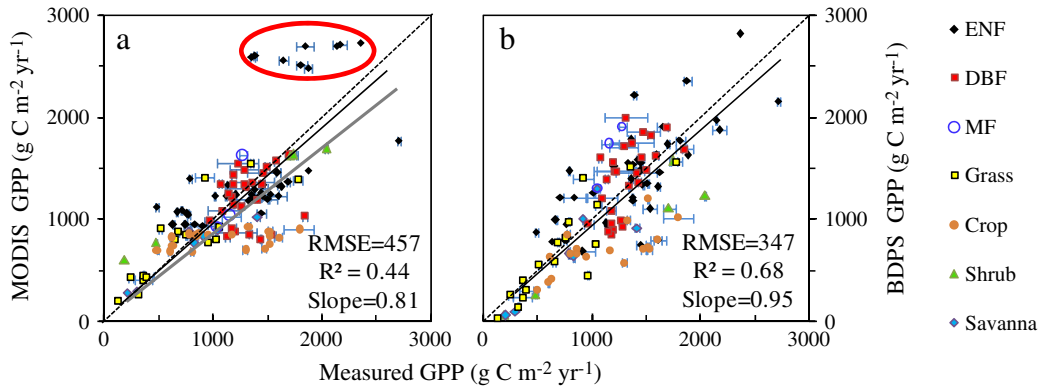
Fig. 2. Comparisons of annual gross primary productivity (GPP) estimated by the MODIS algorithm (left) and the BEPS model (right) against measured GPP (mean ± SE) at eddy-covariance sites during 2000–2005. The dashed line is the 1:1 line and the solid and thin line is the regression line for all 120 site-years at 40 sites. Dots in Red circles (2a) are values of SP1, SP2, and SP3 sites simulated by the MODIS algorithm in the subtropical climate zone. The grey, thicker solid line is the regression line for the rest of the 111 site-years without consideration of values at the SP1, SP2, and SP3 sites. Model performances are assessed using root mean square error (RMSE) with units of g C m^{-2} yr^{-1}, slope, and coefficient of determination (R^2). All statistics are significant at the 0.01 level. ENF: evergreen needleleaf forest; DBF: deciduous broadleaf forest; MF: mixed forest.

square error (RMSE), and relative error (RE) were used to evaluate the performance of models. RE was calculated as:

$$RE = \frac{1}{n}\sum_{i=1}^{n}\left(\frac{\text{Calculated GPP}_i - \text{Measured GPP}_i}{\text{Measured GPP}_i}\right) \times 100\%, \qquad (4)$$

where n is the number of samples. Our approach in this analysis was to compare modeled MODIS and BEPS estimates of GPP against each other and also with observed values from micrometeorological flux towers.

4. Results

4.1. Monthly GPP assessment

Comparisons of monthly GPP from MODIS and BEPS against EC-measured GPP for different land cover types indicated that both models can capture the monthly variability well at most of the sites. However, BEPS, with lower or similar SEs, but always higher R^2 ($p<0.01$), performed better than the MODIS algorithm that had an obvious tendency for biases (Fig. 1).The R^2 between MODIS and EC-measured GPP ranged from 0.46 in croplands to 0.78 in shrubs and savannas, which were lower than the corresponding values between BEPS and EC-measured GPP, which ranged from 0.62 in needleleaf forests to 0.83 in mixed forests. MODIS underestimated EC-measured monthly GPP at high GPP but overestimated EC-measured monthly GPP at low GPP. This bias existed for all cover types and was particularly pronounced for broadleaf forests and croplands (Fig. 1a and d). MODIS performed in needleleaf forests better than other biome types, but it still underestimated about 26% of monthly GPP values during higher productive months. Conversely, it overestimated all months at three needleleaf forest sites (SP1, SP2, and SP3) in the subtropical climate zone. BEPS GPP showed little bias and was on average within of the EC-measured GPP, except in croplands (slope = 0.63, $p<0.01$). In this cover type, BEPS underestimated about 40% of the monthly GPP in summer. This bias was evident in particular in irrigated crops (e.g., Ne1, Ne2, and Ne3 sites, Fig. 1d). BEPS performed best in forests but had larger variances in broadleaf forests, with a RMSE value of 69 g C m^{-2} month^{-1} (Fig. 1b2) and an overestimation of 10% in mixed forests during few months(Fig. 1c2).

4.2. Annual GPP assessment

The overall comparisons of annual GPP across 40 sites also showed that BEPS yielded higher R^2 and lower REs than MODIS (i.e., MODIS: R^2 = 0.47, RMSE = 384 g C m^{-2} yr^{-1} versus BEPS: R^2 = 0.68, RMSE = 347 g C m^{-2} yr^{-1}, $p<0.01$). Because the underestimation of MODIS GPP in highly productive months was offset by overestimation in low-productive months, the variance of annual MODIS GPP values was smaller. When the data at three evergreen needleleaf forest sites (i.e., SP1, SP2, and SP3) were excluded from the analysis, MODIS GPP underestimated at high productivity and overestimated at low productivity (MODIS GPP = 0.33 × EC-measured GPP + 806, R^2 = 0.64, $p<0.01$) (Fig. 3a). On average, BEPS simulated GPP within 5% of EC-measured GPP (slope = 0.95, $p<0.01$). However, BEPS slightly underestimated about 21% of the annual estimated GPP at the lower productivity sites, such as over croplands, shrublands, and savannas, where MODIS overestimated GPP.

Similar patterns in the differences between MODIS GPP and EC-measured GPP are found across different ecosystem types (Figs. 2 and 3). MODIS explained 39%, 68%, and 78% of the variance of annual GPP in needleleaf forests, grasslands, and shrub–savanna lands, respectively, but failed to explain the variance in broadleaf forests and croplands (R$^2 \leq 0.10$). BEPS generally produced higher R^2 values and lower SEs than MODIS algorithm for the corresponding cover types (Fig. 3b). MODIS GPP overestimated GPP in evergreen needleleaf forest sites (SP1, SP2, and SP3) by 47% (these values are shown in circles in Fig. 3a). When these sites were excluded, MODIS algorithm still captured little of the variability of observed values at the needleleaf forest sites and underestimated/overestimated 25% of GPP at a high/low end (Fig. 3a1). BEPS GPP for needleleaf forests was distributed randomly around a 1:1 line against EC-measured GPP. In broadleaf forests, MODIS GPP underestimated measured GPP in some years (Fig. 3b) while BEPS overestimate GPP in some years. MODIS and BEPS GPP were underestimated by about 40-50% (Fig. 3c) at crop sites. This was because both models largely underestimated monthly GPP and failed to capture the monthly patterns at no-till, irrigated maize–soybean rotation Ne1, Ne2, and Ne3 sites (Fig. 1d). In particular, MODIS GPP did not show any annual variability and was practically constant at around ~800 ± 264 g C m^{-2} yr^{-1}.

Fig. 1. Comparisons of monthly gross primary productivity (GPP) estimated by the MODIS algorithm (left) and the BEPS model (right) against measured GPP (mean ± SE) at 40 AmeriFlux sites during 2000–2005. Both MODIS and BEPS outputs at ~1 km resolution were averaged within a 0.05° cell centered over each flux tower location for each month and year. Blue square dots in Fig. 1 are values for SP1, SP2, and SP3 sites and the thick solid line is the regression line without consideration of SP1, SP2, and SP3 sites. Model performances are assessed using root mean square error (RMSE) with units of g C m^{-2} month^{-1}, slope and coefficient of determination (R^2). The AmeriFlux sites are described in Table 1. The dashed line is the 1:1 line and the solid line is the regression line. All statistics are significant at the 0.01 level. NF: needleleaf forest; BF: broadleaf forest; MF: mixed forest; Others: shrub and savanna.
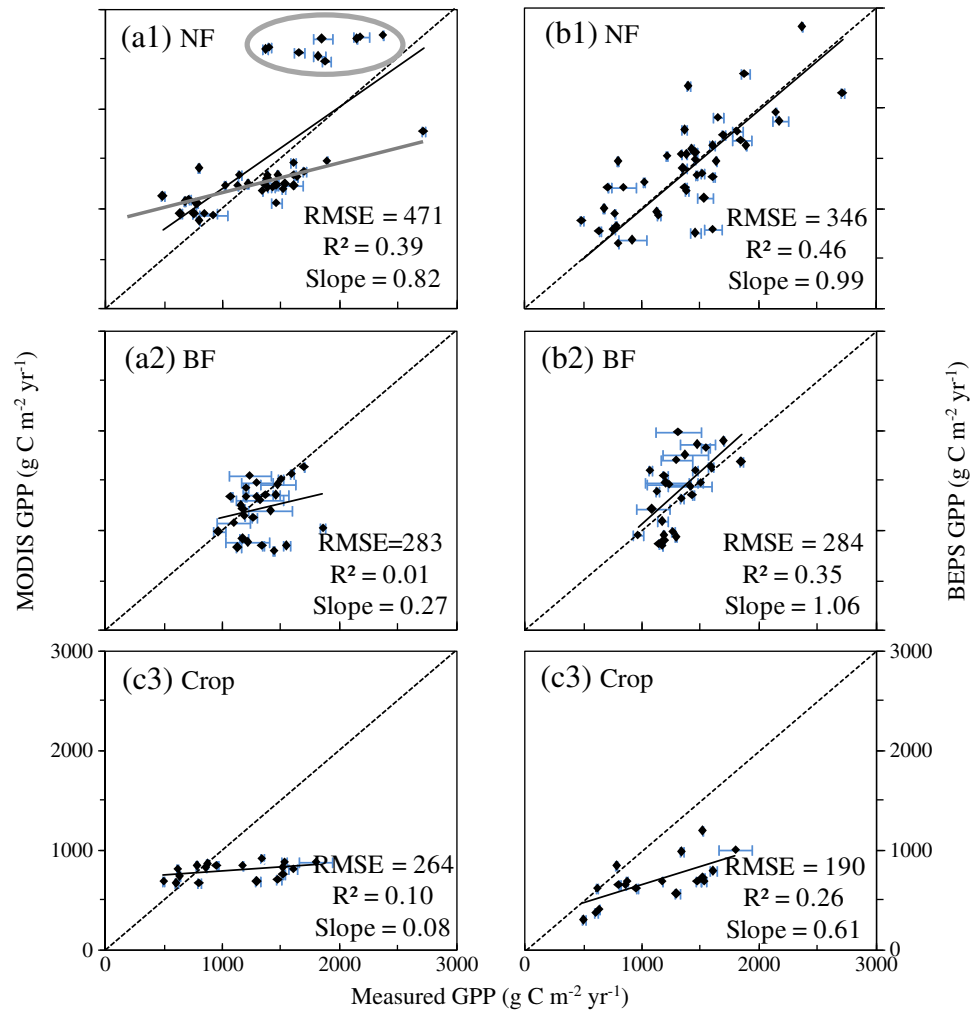
Fig. 3. Same as Fig. 2 but for three separated land cover types. Dots in grey thick circles in Fig. 3(a) are the values of the SP1, SP2, and SP3 sites simulated by the MODIS algorithm in the subtropical climate zone. The grey, thicker solid line is the regression line for the rest of the site-years without consideration of values at the SP1, SP2, and SP3 sites. Model performances are assessed using root mean square error (RMSE) with units of g C m^{-2} yr^{-1}, slope, and coefficient of determination (R^2). All statistics are significant at the 0.01 level. NF: needleleaf forest; BF: broadleaf forest. For illustrative clarity, measured value $\pm$ SE.

In general, the comparisons between modeled and observed annual GPP showed biases similar to those found with monthly MODIS GPP (i.e., overestimate at the low GPP end and underestimate at high end). The differences between MODIS GPP and EC-derived GPP were much larger than the uncertainties of EC-derived GPP. Although the underestimation in summer could be offset by overestimation in other seasons, the annual MODIS GPP tended to be clustered towards certain values regardless of the variance of observations.

The failure of MODIS to represent monthly and annual variability in GPP may be associated with the inadequacy of the LUE models in capturing changes in canopy physiology over time. Biases in MODIS GPP relative to observations arise from a lack of sensitivity to canopy density, which is spatially and temporally variable. Consequently, MODIS GPP is lower than observed values during the growing season because the contribution of shaded leaves to canopy photosynthesis is under-represented. Conversely, unrealistically high GPP during the dormant season is associated with overestimation of the shaded leaf contribution (Sprintsin et al., 2012). These factors might be responsible for large variability in the spatio-temporal distribution of GPP, but they are not accounted for in the LUE modeling approach.

4.3. Continental GPP comparison

The spatial patterns of the average annual GPP estimated by both models across the continental U.S. from 2000 to 2005 were generally consistent (Fig. 4). The highest GPP were found in the north, south, and Pacific Coast regions with values of ~2000–3000 g C m^{-2} yr^{-1}. The lowest GPP (<500 g C m^{-2} yr^{-1}) were found in the Rocky Mountain and Great Plain regions. BEPS GPP was slightly higher than the MODIS GPP in most areas of the north and south regions, while it was lower in the Rocky Mountain and Great Plain regions (Fig. 4). The total GPP from MODIS was larger than BEPS GPP by ~0.42 Pg C yr^{-1} in the Rocky Mountain and Great Plain regions.

Our pixel-by-pixel comparisons between annual modeled GPP, showed that the spatial patterns in MODIS GPP were consistent with those observed at the site-level (Fig. 5). However, annual MODIS GPP was higher in low productivity pixels and lower in high productivity pixels than BEPS GPP. The larger systematic differences between MODIS and BEPS occurred in more clumped canopies (e.g., forests) and in canopies with large monthly variability (e.g., croplands). The average annual MODIS GPP was lower than BEPS GPP in needleleaf and broadleaf forests (34% and 39% less, respectively) and in croplands with high productivity (56% less). In contrast, annual MODIS GPP was 50% higher than BEPS GPP in croplands with low annual productivity.

The comparison of the six-year average between MODIS and BEPS GPP for the continental U.S. showed that the differences between monthly MODIS GPP and BEPS GPP exhibited a double-peak curve (Fig. 6). MODIS GPP was larger than BEPS GPP from September to late spring (e.g., April–May), with two peaks around April and October. MODIS-GPP was lower than BEPS GPP during the summer months. On

Table 2
Site descriptions including site ID, latitude, longitude, vegetation types, available data periods, and references.

ID	Latitude	Longitude	Vegetation types	Period	References
Blo	38.8953	−120.633	ENF	2000–2005	Goldstein et al. (2000)
Ho1	45.2041	−68.7402	ENF	2000–2004	Hollinger et al. (2004)
Ho2	45.2091	−68.747	ENF	2000–2004	Hollinger et al. (2004)
Me2	44.4523	−121.557	ENF	2002–2005	Irvine et al. (2007)
Me3	44.3154	−121.608	ENF	2004–2005	Irvine et al. (2007)
Me5	44.4372	−121.567	ENF	2000–2002	Irvine et al. (2007)
NC1	35.8115	−76.7115	ENF	2005	Noormets et al. (2010)
NC2	35.8031	−76.6679	ENF	2005	Noormets et al. (2010)
NR1	40.0329	−105.546	ENF	2000–2005	Monson et al. (2005)
SP1	29.7381	−82.2188	ENF	2001–2005	Powell et al. (2008)
SP2	29.7648	−82.2448	ENF	2000–2004	Powell et al. (2008)
SP3	29.7548	−82.1633	ENF	2001–2004	Powell et al. (2008)
Wrc	45.8205	−121.952	ENF	2000–2004	Paw et al. (2004)
KS2	28.6086	−80.6715	EBF	2000–2005	Dore et al. (2003)
Bar	44.0646	−71.2881	DBF	2004–2005	Jenkins et al. (2007)
Ha1	42.5378	−72.1715	DBF	2002–2005	Urbanski et al. (2007)
MMS	39.3232	−86.4131	DBF	2000–2005	Dragoni et al. (2007)
MOz	38.7441	−92.2	DBF	2004–2005	Gu et al. (2007)
Oho	41.5545	−83.8438	DBF	2004–2005	Noormets et al. (2008)
UMB	45.5598	−84.7138	DBF	2001–2004	Curtis et al. (2002)
WCr	45.8059	−90.0799	DBF	2000–2005	Cook et al. (2008)
LPH	42.5419	−72.185	MF	2002–2005	Hadley et al. (2008)
Syv	46.242	−89.3477	MF	2002–2005	Desai et al. (2005)
SO4	33.3844	−116.64	Shrub	2004–2005	Luo et al. (2007)
FR2	29.9495	−97.9962	Savanna	2004–2005	
SRM	31.8214	−110.866	Savanna	2004–2005	Scott et al. (2009)
Ton	38.4316	−120.966	Savanna	2001–2005	Ma et al. (2007)
Bkg	44.3453	−96.8362	Grass	2004–2005	
FPe	48.3077	−105.102	Grass	2000–2005	
Goo	34.2547	−89.8735	Grass	2002–2005	
Var	38.4067	−120.951	Grass	2001–2005	Ma et al. (2007)
Wkg	31.7365	−109.942	Grass	2004–2005	Scott et al. (2010)
Wlr	37.5208	−96.855	Grass	2002–2004	Coulter et al. (2006)
ARM	36.6058	−97.4888	Crop	2003–2005	
Bo1	40.0062	−88.2904	Crop	2002–2005	Hollinger et al. (2005)
Ne1	41.1651	−96.4766	Crop	2001–2005	Verma et al. (2005)
Ne2	41.1649	−96.4701	Crop	2001–2005	Verma et al. (2005)
Ne3	41.1797	−96.4396	Crop	2001–2005	Verma et al. (2005)
Ro1	44.7143	−93.0898	Crop	2004–2005	
Ro3	44.7217	−93.0893	Crop	2004–2005	

ENF: evergreen needleleaf forest; EBF: evergreen broadleaf forest; DBF: deciduous broadleaf forest; MF: mixed forest.

average, the total MODIS GPP from May to September was 0.42 Pg C yr^{-1} lower than the corresponding BEPS GPP. The average total MODIS GPP from October to April was 0.88 Pg C yr^{-1} larger than the corresponding BEPS GPP. Consequently, both the annual average and total MODIS GPP for the conterminous U.S. during the period from 2000 to 2005 were 6.6% larger than BEPS GPP (726 g C m^{-2} yr^{-1} and 6.04 Pg C yr^{-1} vs. 779 g C m^{-2} yr^{-1} and 6.46 Pg C yr^{-1}).

5. Discussion

The basis of LUE models is the initial linear relationship between canopy GPP and APAR at low levels of light and for well-watered crop species (Montieth, 1972). In the LUE-based MODIS algorithm, a simple lookup table (LUT) approach is used to assign a constant LUE$_{max}$ for a given biome type and adjusted downward based on VPD and T$_{min}$ stress scalars (Heinsch et al., 2006; Turner et al., 2003). However, the relationship between GPP and APAR is not linear at individual leaf level and is characterized by spatial–temporal heterogeneity associated with various illumination levels. There are, therefore, issues associated with the use of the biome-dependent constant LUE$_{max}$ and the LUE-based model's ability to capture the spatial and temporal variability of GPP by using meteorological scalars (Zhao & Running, 2010). Several studies suggested different schemes to downscale pre-assigned LUE$_{max}$ values using meteorological observations (Heinsch et al., 2006; Turner et al.,

2006; Yang et al., 2007) or surface remote sensing observations (Drolet et al., 2008; Hilker et al., 2008; Wu et al., 2012). However, all these models do not account for the difference in LUE between sunlit and shaded leaves (Hilker et al., 2008). Because GPP can vary greatly in space and time as result of the variability in sunlit and shaded leaf fraction, we argue that scaling LUE$_{max}$ without considering this factor greatly limits the LUE-based model performances.

The performances of one-leaf and two-leaf schemes were recently evaluated against 8 tower flux sites in North America using the BEPS model (Sprintsin et al., 2012). It was found that the one-leaf scheme produces negatively biased GPP results by about 40–60% compared with EC observations when realistic leaf-level parameters (V$_{cmax}$ and J$_{max}$) are used. The biases are mostly caused by excluding the contribution of shaded leaves. By testing the response of both schemes to changes in shaded leaf fraction, the results showed that the contribution of the shaded leaves to the total simulated productivity can be as high as 70% for highly clumped stands and seldom decreases below ~40% for less-clumped canopies. When the leaf-level parameters are inflated more than two times to force the big-leaf model to agree with observed GPP, the model results have the tendency to be biased in the same way as LUE models at the high and low ends of GPP.

Two-leaf models represent an improvement over LUE models because they express the canopy-level photosynthesis rate as the sum of the contributions from sunlit and shaded leaves, acknowledging that the internal physiological processes of these two leaf groups are substantially different (Fig. 7). Photosynthesis in sunlit leaves is often light-saturated, resulting in a lower LUE. Photosynthesis in shaded leaves is often non light-saturated and essentially has a linear response to APAR, resulting in a higher LUE (Chen et al., 1999; Dai et al., 2004; De Pury & Farquhar, 1997; Norman, 1980; Wang & Leuning, 1998). At leaf level, sunlit leaves are mostly limited by the level of Rubisco activities related to leaf nutrient conditions and the ambient temperature (Farquhar et al., 1980; also see Appendix A). Shaded leaves are mostly limited by the electron transport related to the level of incident radiation. Consequently, two-leaf models have the ability to simulate the difference in the biochemical processes between sunlit and shaded leaves and thereby capture spatio-temporal variations in these processes.

The separated contributions to total GPP of sunlit and shaded leaves simulated by BEPS (Fig. 7) indicate that sunlit leaves contribute to a large proportion of the total GPP at low productivity or low LAI. However, the contributions of shaded leaves become significant at high productivity or high LAI (Fig. 7). Our results show that BEPS simulates GPP with considerable error (Fig. 1). Nevertheless, the estimation of the shaded leaf area as a function of LAI is based on well-established physics (Eqs. A7a and A7b): the maximum sunlit LAI is 2 for a spherical leaf angle distribution (G(θ) = 0.5) and the shaded LAI increases with total canopy LAI. At low LAI values, where the shaded leaf fraction is small, LUE models would overestimate GPP because they calculate the fraction of shaded leaf based on the mean LAI for the biome. This may explain the higher annual MODIS GPP in low LAI areas such as western Nebraska, Kansas, and North and South Dakota (Fig. 4). By the same argument, GPP estimated by LUE models would be lower at high LAI areas because the estimated fraction of shaded leaves, based on biome mean conditions, would be lower than the actual fraction. For example, annual MODIS GPP is 20% lower than BEPS GPP in 2003 (Fig. 7). This may explain the systematic errors at the two ends of the modeled GPP range relative to observations (Fig. 1), and the dampened monthly and annual variations simulated by the LUE-based MODIS algorithm (Figs. 1–2).

The clumping of leaves, in both natural canopy structures and human-made crop rows, causes more overlapping of leaves than in the random leaf distribution. Hence, the fraction of the shaded leaves for the same LAI is much larger in clumped canopies than in random canopies (Baldocchi & Harley, 1995; Chen et al., 2005). BEPS has also been applied to the global terrestrial biosphere with consideration of the clumping effect (Chen et al., 2012). They found that shaded leaves contribute 50%, 38%, 37%, 39%, 26%, 29% and 21% to the total GPP for broadleaf evergreen
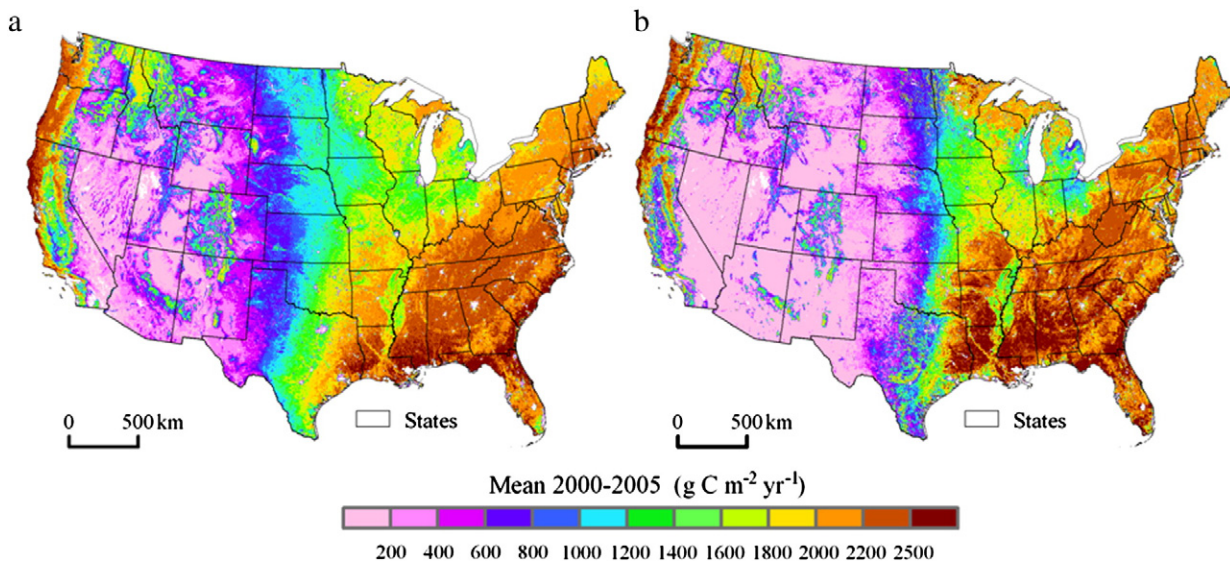
Fig. 4. The spatial distributions of annual gross primary productivity (GPP) over the conterminous U.S. by (a) the MODIS algorithm and (b) the BEPS model.

forest, broadleaf deciduous forest, evergreen conifer forest, deciduous conifer forest, shrub, C4 vegetation, and other vegetation, respectively. Since leaves in forests are often highly clumped, resulting in larger contributions of shaded leaves to the total GPP than canopies with random leaf spatial distributions, the biases in GPP estimation for forests are thus expected to be particularly large in clumped canopies. This is supported by the results for needleleaf and broadleaf forests (Fig. 5). LUE models essentially treat the entire canopy as a single unshaded leaf characterized by a single LUE and still represent the canopy with a non-realistic random-distribution of leaves. Because of this, LUE models may not adequately simulate the spatial and temporal variations caused by the clumping of leaves. Similarly, canopies with large monthly variations of LAI, such as crops, are expected to have large variation in the contribution

of shaded leaves to GPP, resulting in potential large biases at the low and high ends of GPP (Figs. 1 and 3). Both MODIS GPP algorithm and BEPS performed poorly at crop sites, especially at irrigated sites (Fig. 1). This suggests that irrigation and fertilization practices, and in general differences among crop types, may be more critical than canopy structure in determining model performances.

An example of model comparison for GPP in 2003 (Figs. 8 and 9) shows that the MODIS annual GPP is larger than BEPS annual GPP when GPP of all shaded leaves is lower than the average. Conversely, MODIS annual GPP is smaller than the corresponding BEPS results when GPP of shaded leaves is larger than the average. Since the underlying assumption of LUE models is constant shaded leaf contributions to the total GPP, these models are liable to cause the opposite biases at the
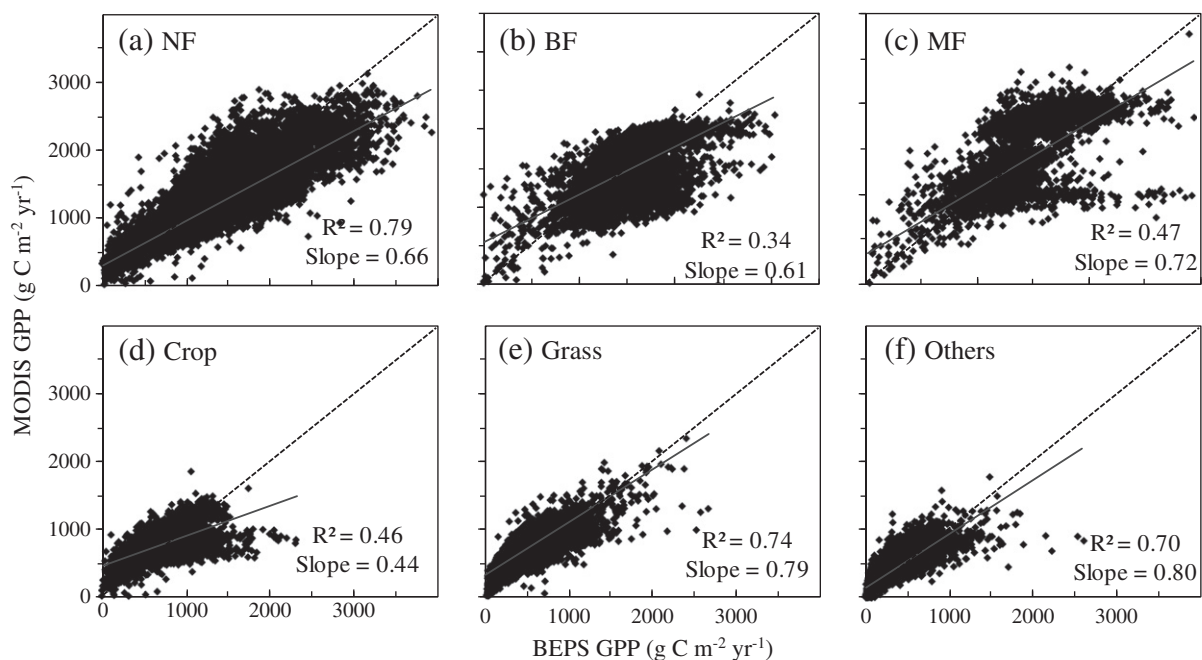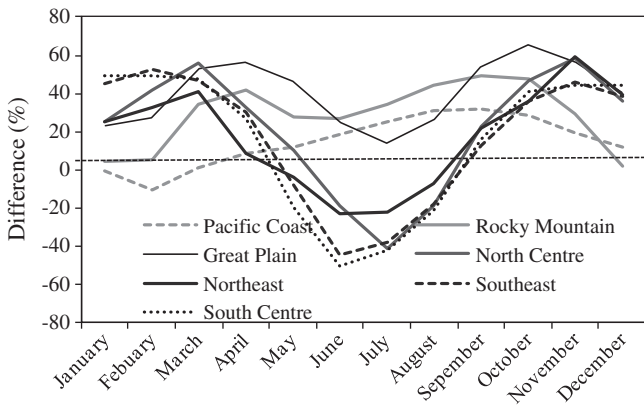

Fig. 5. Pixel-by-pixel comparisons of annual gross primary productivity (GPP) estimated by the MODIS algorithm and the BEPS model for different land cover types across the conterminous U.S. in 2003. The dashed line is the 1:1 line and the solid line is the regression line. Considering the overloading pixel numbers at 1 km resolution, the simulated GPP by both MODIS and BEPS are aggregated from ~1 km pixels to 0.05° grids. Due to the differences between GLC2000 and MODIS land cover classifications, we only compared the grids with the same land cover in both classifications. Model performances are assessed using root mean square error (RMSE) with units of g C m^{-2} yr^{-1}, and coefficient of determination (R^2). All statistics are significant at the 0.01 level. NF: needleleaf forest; BF: broadleaf forest; MF: mixed forest; Others: shrub and savanna.

Fig. 6. Percent differences in average annual gross primary productivity (GPP) estimated by the MODIS algorithm against the BEPS model for different regions across the conterminous U.S. during 2000–2005.

low and high ends of GPP values (either the total or shaded leaf GPP). Compared with BEPS, MODIS GPP is lower by ~200 g C m^{-2} yr^{-1} when the contribution of shaded leaves is larger than 400 g C m^{-2} yr^{-1}. Conversely, MODIS GPP is overestimated by ~150 g C m^{-2} yr^{-1}, on average, when the contribution of shaded leaves is more than 400 g C m^{-2} yr^{-1} (Fig. 8).

The spatial distribution of the differences between MODIS GPP and BEPS GPP corresponds with variation in the contribution of shaded leaves to total GPP (Fig. 9). In Washington, north Idaho, Wisconsin, New York, and Maine, where LAI is large (>5, Fig. 7d), shaded leaves contribute 65% of the total annual GPP (Fig. 9a). In such conditions, MODIS GPP is significantly (~35%) lower than BEPS GPP, owing to the

assumption of the constant contribution from shaded leaves (Fig. 9b). On the other hand, for areas with small LAI values (LAI<1) such as the Rocky Mountain region, the contribution of shaded leaves is on average<20% of the total annual GPP. Therefore, MODIS GPP in these areas calculated based on LUE$_{max}$ values representing the mean conditions of the biomes is found to be 50%–200% larger than BEPS GPP (the relative differences are large because the absolute GPP values are small). Although shaded leaves contribute half of the total annual GPP in the southeast region, such as Alabama, the MODIS algorithm still underestimates by about 15% of the total annual GPP relative to the BEPS model. In contrast, in the Mid-Atlantic region, such as West Virginia, shaded leaves contribute ~65% of the total annual GPP but the differences in GPP between MODIS and BEPS are relatively small (<10%). The underlying mechanism for such differences in agreement among simulated values is still not well-understood and we suggest that the contribution of shaded leaves could probably be offset by T$_{min}$ and VPD adjustments in the MODIS algorithm. Therefore, further analysis is especially needed on the combined impacts of various factors (e.g. canopy structure, temperature, water content, etc.) that can influence GPP, which help in both explaining the differences among model simulations and in developing future GPP algorithms.

Factors other than within-canopy radiation transfer also probably cause measured LUE and GPP to depart from modeled estimates. Martin and Jokela (2004) showed that loblolly and slash pine LUE varied by a factor of two over space and time in a long term replicated experiment, with variation caused by both soil nutrient availability (fertilized vs. non-fertilized treatments) as well as changes associated with stand development and aging. Other studies have also shown that misrepresentation of the seasonal cycle resulted in over-prediction of GPP during the spring and autumn transition period by 160 ± 154, 75 ± 130 g C m^{-2} yr^{-1}, respectively (Richardson et al., 2012).
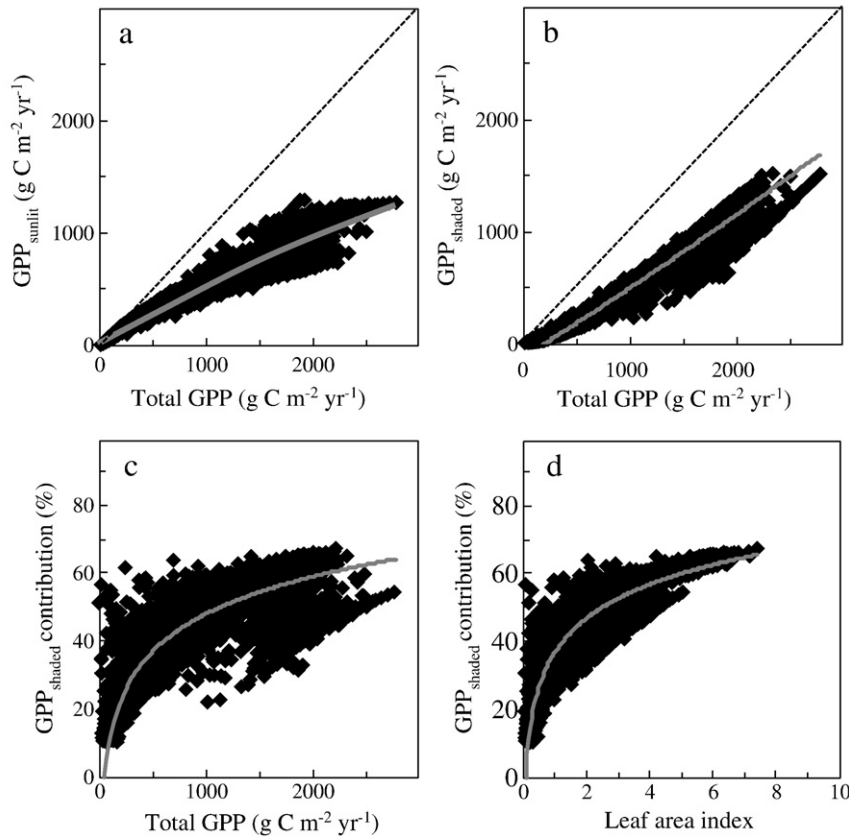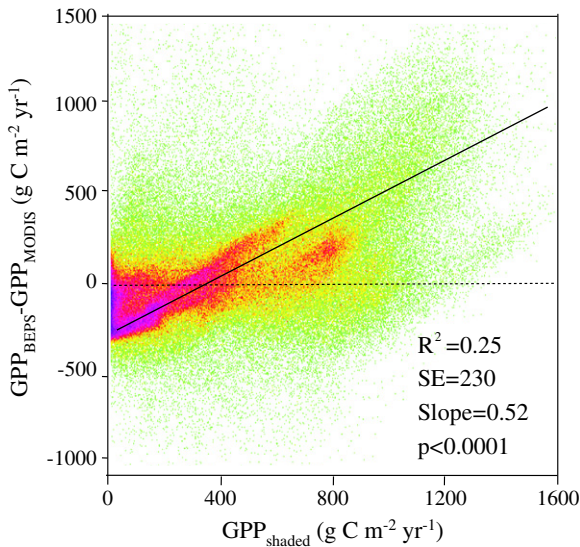

Fig. 7. Pixel-by-pixel comparisons of (a–b) annual gross primary productivity (GPP) of sunlit and shaded leaves against the total annual GPP and (c–d) relative contribution of shaded leaves against the total annual GPP and leaf area index (LAI) in needleleaf forests estimated by the BEPS model across the conterminous U.S. in 2003. Contributions of sunlit and shaded leaves to the total annual GPP and LAI in other vegetation types are similar to the patterns of the needleleaf forests.

The purpose of this study was not to demonstrate that process-based models with separation of shaded and sunlit leaves perform necessarily better than LUE models in all contexts and application. We fully recognize that LUE models have the advantage of simplicity and are suitable for many purposes, as well as that uncertainty and prediction errors can be also associated with the parameterization of more 'complex' process-based models. However, we believe that the critical contribution of this work largely resides in recognizing one of the major shortcomings of LUE models, and providing directions for further improvements. For instance, reduction in GPP estimates errors could be achieved by either developing a two-leaf LUE model or allowing LUE_{max} to vary spatially and temporally as a function of LAI or other canopy structural attributes.

6. Conclusion

In this study, GPP simulated by the LUE-based MODIS algorithm and the two-leaf process-based BEPS model were examined against EC measurements at 40 AmeriFlux sites from 2000 to 2005. Both models produced comparable mean GPP values for the conterminous U.S. landmass. However, the spatial and temporal patterns of the estimated GPP differ considerably. Compared with monthly or annual EC-derived GPP values, BEPS performed better than the MODIS algorithm, although both methods underestimated GPP at crop sites. The MODIS algorithm underestimated GPP at high productivity and overestimated GPP at low productivity. The largest biases occurred in clumped canopies, such as forests, and in canopies with large monthly variability, such as crops. These biases were generally not found or were less pronounced with the two-leaf BEPS model. Our results suggest that the major reason for the absence of strong biases in the BEPS results resides in the explicit treatment of the contribution of shaded/sunlit leaves to the calculation of total GPP and recognition in the model of different physiological attributes of sun and shaded leaves. In BEPS, the relative contribution from shaded leaves to total GPP is small for vegetation characterized by low LAI and low productivity, and large in vegetation with high LAI and productivity. In the MODIS algorithm, one single value for LUE, representing the mean condition for a particular type of vegetation, is used. This causes the overestimation of the effect of shaded leaves at low LAI, and the underestimation at high LAI.

Fig. 8. Pixel-by-pixel comparisons of GPP differences (ΔGPP; g C m^{-2} yr^{-1}) between BEPS and MODIS against the annual GPP of shaded leaves over the conterminous U.S. in 2003. ΔGPP = GPP$_{BEPS}$ − GPP$_{MODIS}$. Colors represent the distribution density (increasing from green to red). The performance is assessed using root mean square error (RMSE) with units of g C m^{-2} yr^{-1}, slope, and coefficient of determination (R^2). Solid line is the linear trend line, and dot line is 'zero' value line.

These biases in the LUE-based MODIS algorithm at the low and high ends of GPP, found through comparison with observations and estimates by a process-based model, are shown to produce considerable distortions in the spatial and temporal distribution patterns of GPP over the conterminous U.S. landmass. The amount of the disagreement is found to be highly correlated with the contribution of shaded leaves to GPP. As LUE models found many more applications due to their relatively low requirement in parameterization, it is equally important to recognize their potential limitations as a ways, among others, to improve their reliability.

Appendix A. BEPS principles

A.1. Leaf photosynthesis

The leaf photosynthetic rate (A) is assumed to be limited by the Rubisco-limited rate of CO_2 assimilation (W_c) and the electron transport-limited rate of CO_2 assimilation (W_j).

$$W_c = \begin{cases} V_m \dfrac{C_i - \Gamma}{C_i + k_{co}} & \text{for } C_3 \\ V_m & \text{for } C_4 \end{cases}, \tag{A1}$$

$$W_j = \begin{cases} J \dfrac{C_i - \Gamma}{4.5 C_i + 10.5\Gamma} & \text{for } C_3 \\ J & \text{for } C_4 \end{cases}, \tag{A2}$$

$$\theta_1 J^2 - (I_{le} + J_m)J + I_{le}J_m = 0, \tag{A3}$$

$$A = \min(W_c, W_j) - R_d, \tag{A4}$$

$$A_{canopy} = A_{sun}L_{sun} + A_{shade}L_{shade}, \tag{A5}$$

where W_c is photosynthetic rate limited by Rubisco activities; W_j is photosynthetic rate limited by electron transport; C_i is the atmospheric CO_2 concentration; Γ is CO_2 compensation point; k_{co} is coefficient associated with enzyme kinetics; V_m is photosynthetic Rubiso capacity per unit leaf area; J is the rate of electron transport rate per unit leaf area; θ_1 is irradiance; I_{le} is PAR effectively absorbed by PSII per unit leaf area; J_m is potential rate of electron transport rate per unit leaf area; A is the net photosynthetic rate; R_d is daytime leaf dark respiration; L is the leaf area index; the subscripts 'sunlit', 'shaded' and 'canopy' denote the photosynthesis and LAI of sunlit leaves, shaded leaves and canopy (Chen et al., 1999; De Pury & Farquhar, 1997).

A.2. Sunlit and shaded LAI stratification

For daily estimation, leaves are often grouped into various sub-canopy structures making the leaf spatial distribution non-random, therefore the assumption of random leaf spatial distribution is generally seriously violated (Chen, 1996).The effect of this non-randomness on radiation transmission through an azimuthally symmetric canopy has been described using a leaf dispersion parameter Ω (Nilson, 1971)

$$P(\theta) = e^{-G(\theta)\Omega L/\cos\theta}, \tag{A6}$$

a

b
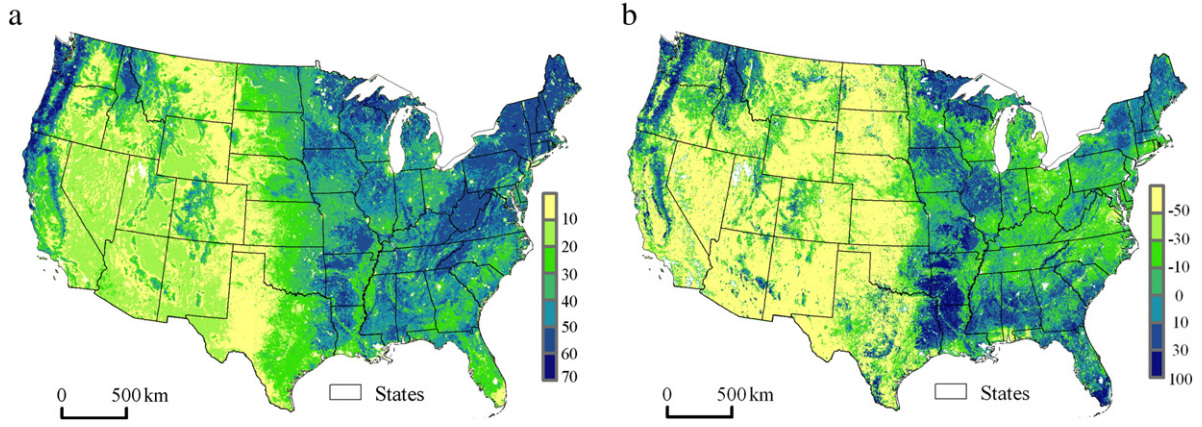
Fig. 9. Spatial distributions of (a) the contribution (%) of shaded leaves to the total annual gross primary productivity (the ratio of annual GPP of shaded leaves to total annual GPP) estimated by the BEPS model and (b) differences (%) of annual GPP estimated by the MODIS algorithm against the BEPS model ($=(GPP_{BEPS} - GPP_{MODIS})/GPP_{BEPS}$) over the conterminous U.S. in 2003.

where $P(\theta)$ is the probability of radiation transmission through the canopy at zenith angle θ, $G(\theta)$ is the projection coefficient and often taken as 0.5 for the random (spherical) leaf angle distribution, and L is the LAI. Clumping effectively reduces the influence of LAI on radiation interception, and therefore the Ω value is usually smaller than unity. Ω is therefore often called as clumping index (Chen, 1996).

For a given canopy structure as described by L and Ω, the total LAI (L) can be separated into sunlit LAI (L_{sun}) and shaded LAI (L_{shade}) for the purpose of canopy-level photosynthesis modeling using a two-leaf model. The method of Norman (1982) has been modified to consider the effect of foliage clumping on the sunlit and shaded LAI separation (Chen et al., 1999):

$$L_{sun} = \frac{\cos\theta(1 - \exp(-G(\theta)L\Omega/\cos\theta))}{G(\theta)}, \tag{A7a}$$

$$L_{shade} = L - L_{sun}. \tag{A7b}$$

A.3. Sunlit and shaded leaf irradiance

Two-leaf models are shown to be effective in modeling canopy-level photosynthetic rate (De Pury & Farquhar, 1997; Wang & Leuning, 1998) than "big-leaf" photosynthesis models. The methodology developed by Chen et al. (1999) for computationally efficient estimation of sunlit and shaded leaf irradiances is used in this study. In this methodology, a simple model developed by Norman (1982) for estimating the multiply scattered irradiance in the canopy is adjusted for clumping for diffuse irradiance estimation.

A.4. Stomatal conductance

Using Leuning's method, the photosynthesis rate of a leaf can be estimated using Farqhuar's model once the stomatal conductance of the leaf is known. Ball (1988) found that leaf stomatal conductance is found to be linearly related to its photosynthetic rate (A, presenting either A_{sun} or A_{shade}):

$$g = m\frac{Ah_s}{C_s}p + b, \tag{A8}$$

where g is stomatal conductance, m is a plant species dependent coefficient (Table A1), h_s is the relative humidity at the leaf surface, p is the atmospheric pressure, C_s is the CO_2 concentration at the leaf surface, and b is a small value due to leaf dark respiration (Table A1). Eq. (A8) is often called Ball–Berry equation. However, the important influences of soil water on g and A are not mechanistically included in the original

Ball–Berry formulation (Eq. A8). Following Ju et al. (2006), we modify it as follows:

$$g = f_w\left(m\frac{Ah_s}{C_s}p + b\right), \tag{A9}$$

where f_w is a soil moisture scaling factor. As g is needed in A calculations and A is needed in g calculations, an iteration procedure is usually followed for simultaneous estimations of A and g. We use an analytical solution of g (Baldocchi, 1994) in order to improve the computation efficiency for regional simulations.

A.5. Soil moisture scalar

The root water uptake modeling scheme developed by Ju et al. (2006) is used to calculate f_w in this study. In this scheme, the rate of root water uptake is directly proportional to the soil water availability to roots. The soil water availability factor $f_{w,i}$ in layer i is calculated as:

$$f_{w,i} = \frac{1.0}{f_i(\psi_i)f_i(T_{s,i})}, \tag{A10}$$

where $f_i(\psi_i)$ is a function of matrix suction ψ_i(m) (Zierl, 2001). The effect of soil temperature on soil water uptake $f_i(T_{s,i})$ is described as follows (Bonan, 1991):

$$f_i(T_{s,i}) = \begin{cases} \dfrac{1.0}{1 - \exp\left(t_1 T_{s,i}^{t_2}\right)} & T_{s,i} > 0°C \\ \infty & \text{else} \end{cases}, \tag{A11}$$

where t_1 and t_2 are two parameters determining the sensitivity of water uptake by roots to soil temperature. In this study, $t_1 = 0.02$ and $t_2 = 2.0$.

To consider the variable soil water potential at different depths, we follow the scheme of Ju et al. (2006) to calculate the weight of each layer to f_w:

$$w_i = \frac{R_i f_{w,i}}{\sum_{i=1}^{n} R_i f_{w,i}}, \tag{A12}$$

where R_i is the root fraction in layer i. The overall soil water availability f_w of the whole soil profile is then:

$$f_w = \sum_{i=1}^{n} f_{w,i} w_i. \tag{A13}$$

Table A1
Biochemical and biophysical parameters used for various land cover types in this study.

Parameters	Broadleaf evergreen	Broadleaf deciduous	Evergreen conifers	Deciduous conifers	Shrub	C4 plants	Others	References
V_{cmax} mol m^{-2} s^{-1} (at 25 °C)	29.0 ± 7.7	57.7 ± 21.2	62.5 ± 24.7	39.1 ± 11.7	57.9 ± 19.6	100.7 ± 36.6	90.0 ± 89.5	Wullschleger (1993); Medlyn et al. (1999); Niu et al. (2005); Kattge et al. (2009)
J_{max} μmol m^{-2} s^{-1}	55.1	123.7	135.2	79.2	124.1	193.1	200.0	Wullschleger (1993); Medlyn et al. (1999)
N_0 g m^{-2}	$2.17 + 0.8$	$1.74 + 0.71$	$3.10 + 1.35$	$1.81 + 0.64$	$1.86 + 0.84$	$1.62 + 0.61$	$1.69 + 0.69$	Kattge et al. (2009)
χ_n m^2 g^{-1}	0.48	0.59	0.33	0.56	0.57	0.62	0.60	Kattge et al. (2009)
Slope (m)	8	8	8	8	8	4	8	Ball (1988); Leuning et al. (1995); Medlyn et al. (1999)
Intercept (b), mol m^{-2} s^{-1}	0.0011	0.0011	0.0011	0.0011	0.0011	0.0011	0.0011	Ball (1988); Leuning et al. (1995); Medlyn et al. (1999)

Note: The values of V_{cmax} for the various plant functional types (PFTs), except C4 plants, were adopted from Kattge et al. (2009), who conducted a metadata analysis with 723 leaf-level V_{cmax} data points. The J_{max} values are estimated using the equation established by Medlyn et al. (1999) through a metadata analysis. The values of m for the various PFTs vary in a large range from 5 to 16, but we have chosen the most frequently used values. The intercept values (b) are generally very small and treated as a constant for all PFTs.

References

Baldocchi, D. (1994). An analytical solution for coupled leaf photosynthesis and stomatal conductance models. *Tree Physiology*, 14, 1069–1079.

Baldocchi, D., Falge, E., Gu, L., Olson, R., Hollinger, D., Running, S. W., et al. (2001). FLUXNET: A new tool to study the temporal and spatial variability of ecosystem—Scale carbon dioxide, water vapor, and energy flux densities. *Bulletin of the American Meteorological Society*, 82, 2415–2434.

Baldocchi, D. D., & Harley, P. C. (1995). Scaling carbon dioxide and water vapor exchange from leaf to canopy in a deciduous forest: model testing and application. *Plant, Cell & Environment*, 8, 1157–1173.

Ball, J. T. (1988). An analysis of stomatal conductance. Ph.D. thesis, Stanford University, 89.

Bonan, G. B. (1991). A biophysical surface-energy budget analysis of soil-temperature in the boreal forests of Interior Alaska. *Water Resources Research*, 27, 767–781.

Campbell, G. S., & Norman, J. M. (1998). An introduction to environmental biophysics. New York: Springer-Verlag.

Chen, J. M. (1996). Canopy architecture and remote sensing of the fraction of photosynthetically active radiation absorbed by boreal conifer stands. *IEEE Transactions on Geoscience and Remote Sensing*, 34, 1353–1368.

Chen, J. M., Chen, W., Liu, J., & Cihlar, J. (2000). Annual carbon balance of Canada's forests during 1895–1996. *Global Biogeochemical Cycle*, 14(3), 839–850.

Chen, J. M., Deng, F., & Chen, M. (2006). Automated erratic cubic-spline capping method for reconstructing seasonal trajectories of a surface parameter derived from remote sensing. *IEEE Transactions on Geoscience and Remote Sensing*, 44, 2230–2238.

Chen, J. M., & Leblanc, S. (1997). A 4-scale bidirectional reflection model based on canopy architecture. *IEEE Transactions on Geoscience and Remote Sensing*, 35, 1316–1337.

Chen, J. M., Liu, J., Cihlar, J., & Goulden, M. L. (1999). Daily canopy photosynthesis model through temporal and spatial scaling for remote sensing applications. *Ecological Modelling*, 124, 99–119.

Chen, J. M., Menges, C. H., & Leblanc, S. G. (2005). Global derivation of the vegetation clumping index from multi-angular satellite data. *Remote Sensing of Environment*, 97, 447–457.

Chen, J. M., Mo, G., Pisek, J., Liu, J., Deng, F., Ishizawa, M., & Chan, D. (2012). Effects of Foliage Clumping on the estimation of global terrestrial gross primary productivity. *Global Biogeochemical Cycle*, 26, GB1019, http://dx.doi.org/10.1029/2010GB003996.

Cook, B. D., Bolstad, P. V., Martin, J. G., Heinsch, F. A., Davis, K. J., Wang, W. G., et al. (2008). Using light-use and production efficiency models to predict photosynthesis and net carbon exchange during forest canopy disturbance. *Ecosystems*, 11, 26–44.

Coops, N. C., Ferster, C. J., Waring, R. H., & Nightingale, J. (2009). Comparison of three models for predicting gross primary production across and within forested ecoregions in the contiguous United States. *Remote Sensing of Environment*, 113, 680–690.

Coulter, R. L., Pekour, M. S., Cook, D. R., Klazura, G. E., Martin, T. J., & Lucas, J. D. (2006). Surface energy and carbon dioxide fluxes above different vegetation types within ABLE. *Agricultural and Forest Meteorology*, 136, 147–158.

Curtis, P. S., Hanson, P. J., Bolstad, P., Barford, C., Randolph, J. C., Schmid, H. P., et al. (2002). Biometric and eddy-covariance based estimates of annual carbon storage in five eastern North American deciduous forests. *Agricultural and Forest Meteorology*, 113, 3–19.

Dai, Y., Dickinson, R. E., & Wang, Y. (2004). A two-big-leaf model for canopy temperature, photosynthesis, and stomatal conductance. *Journal of Climate*, 17, 2281–2300.

De Pury, D. G., & Farquhar, G. D. (1997). Simple scaling of photosynthesis from leaves to canopies without the errors of big-leaf models. *Plant, Cell & Environment*, 20, 537–557.

Deng, F., Chen, J. M., Plummer, S., & Chen, M. (2006). Global LAI algorithm integrating the bidirectional information. *IEEE Transactions on Geoscience and Remote Sensing*, 44, 2219–2229.

Desai, A. R., Bolstad, P. V., Cook, B. D., Davis, K. J., & Carey, E. V. (2005). Comparing net ecosystem exchange of carbon dioxide between an old-growth and mature forest in the upper Midwest, USA. *Agricultural and Forest Meteorology*, 128, 33–55.

Dore, S., Hymus, G. J., Johnson, D. P., Hinkle, C. R., Valentini, R., & Drake, B. G. (2003). Cross validation of open-top chamber and eddy covariance measurements of ecosystem CO2 exchange in a Florida scrub-oak ecosystem. *Global Change Biology*, 9, 84–95.

Dragoni, D., Schmid, H. P., Grimmond, C. S. B., & Loescher, H. W. (2007). Uncertainty of annual net ecosystem productivity estimated using eddy covariance flux measurements. *Journal of Geophysical Research*, 112, D17102, http://dx.doi.org/10.1029/2006JD008149.

Drolet, G. G., Middleton, E. M., Huemmrich, K. F., Hall, F. G., Amiro, B. D., Barr, A. G., et al. (2008). Regional mapping of gross light-use efficiency using MODIS spectral indices. *Remote Sensing of Environment*, 112(6), 3064–3078.

Farquhar, G. D., von Caemmerer, S., & Berry, J. A. (1980). A biochemical model of photosynthetic CO2 assimilation in leaves of C3 species. *Planta*, 149, 78–90.

Feng, X., Liu, G., Chen, J. M., Chen, M., Liu, J., Ju, W., et al. (2007). Simulating net primary productivity of terrestrial ecosystems in China using a process model driven by remote sensing. *Journal of Environmental Management*, 85, 563–573.

Foley, J. A., Prentice, I. C., Ramunkutty, N., Levis, S., Pollard, D., Sitch, S., et al. (1996). An integrated biosphere model of land surface processes, terrestrial carbon balance and vegetation dynamics. *Global Biogeochemical Cycles*, 10, 603–628.

Goldstein, A. H., Hultman, N. E., Fracheboud, J. M., Bauer, M. R., Panek, J. A., Xu, M., et al. (2000). Effects of climate variability on the carbon dioxide, water, and sensible heat fluxes above a ponderosa pine plantation in the Sierra Nevada (CA). *Agricultural and Forest Meteorology*, 101, 113–129.

Gu, L., Meyers, T., Pallardy, S. G., Hanson, P. J., Yang, B., Heuer, et al. (2007). Influences of biomass heat and biochemical energy storages on the land surface fluxes and diurnal temperature range. *Journal of Geophysical Research*, 112, D02107, http://dx.doi.org/10.1029/2006JD007425.

Hadley, J. L., Kuzeja, P. S., Daley, M. J., Phillips, N. G., Mulcahy, T., & Singh, S. (2008). Water use and carbon exchange of red oak- and eastern hemlock-dominated forests in the northeastern USA: Implications for ecosystem-level effects of hemlock woolly adelgid. *Tree Physiology*, 28, 615–627.

Haxeltine, A., & Prentice, I. C. (1996). BIOME3: An equilibrium terrestrial biosphere model based on ecophysiological constraints, resource availability, and competition among plant functional types. *Global Biogeochemical Cycles*, 10(4), 693–709, http://dx.doi.org/10.1029/96GB02344.

He, L., Chen, J. M., Pisek, J., Schaaf, C. B., & Strahler, A. H. (2012). Global clumping index map derived from the MODIS BRDF product. *Remote Sensing of Environment*, 119, 118–130.

Heinsch, F. A., Zhao, M., Running, S. W., Kimball, J. S., Nemani, R. R., Davis, K. J., et al. (2006). Evaluation of remote sensing based terrestrial productivity from MODIS using regional tower eddy flux network observations. *IEEE Transactions on Geoscience and Remote Sensing*, 44, 1908–1925.

Hilker, T., Coops, N. C., Hall, F. G., Black, T. A., Wulder, M. A., Nesic, Z., et al. (2008). Separating physiologically and directionally induced changes in PRI using BRDF models. *Remote Sensing of Environment*, 112, 2777–2788.

Hollinger, D. Y., Aber, J., Dail, B., Davidson, E. A., Goltz, S. M., Hughes, H., et al. (2004). Spatial and temporal variability in forest–atmosphere CO2 exchange. *Global Change Biology*, 10, 1689–1706.

Hollinger, S. E., Bernacchi, C. J., & Meyers, T. P. (2005). Carbon budget of mature no-till ecosystem in North Central Region of the United States. *Agricultural and Forest Meteorology*, 130, 59–69.

Houborg, R., Anderson, M. C., Norman, J. M., Wilson, T., & Meyers, T. (2009). Intercomparison of a 'bottom-up' and 'top-down' modeling paradigm for estimating carbon and energy fluxes over a variety of vegetative regimes across the U.S. *Agricultural and Forest Meteorology*, 149, 1875–1895.

Irvine, J., Law, B. E., & Hibbard, K. A. (2007). Postfire carbon pools and fluxes in semiarid ponderosa pine in Central Oregon. *Global Change Biology*, 13, 1748–1760.

Jarvis, P. G. (1976). The interpretation of the variations in leaf water potential and stomatal conductance found in canopies in the fields. *Philosophical Transactions of the Royal Society of London, Series B*, 273, 593–610.

Jenkins, J. P., Richardson, A. D., Braswell, B. H., Ollinger, S. V., Hollinger, D. Y., & Smith, M. L. (2007). Refining light-use efficiency calculations for a deciduous forest canopy using simultaneous tower-based carbon flux and radiometric measurements. *Agricultural and Forest Meteorology*, 143, 64–79.

Ju, W., Chen, J. M., Black, T. A., Barr, A. G., Liu, J., & Chen, B. (2006). Modeling coupled water and carbon fluxes in a boreal aspen forest. *Agricultural and Forest Meteorology*, 140, 136–151.

Jung, M., Vetter, M., Herold, M., Churkina, G., Reichstein, M., Zaehle, S., et al. (2007). Uncertainties of modeling gross primary productivity over Europe: A systematic study

on the effects of using different drivers and terrestrial biosphere models. *Global Biogeochemical Cycles*, 21, GB4021, http://dx.doi.org/10.1029/2006GB002915.

Kattge, J., Knorr, W., Raddatz, T., & Wirth, C. (2009). Quantifying photosynthetic capacity and its relationship to leaf nitrogen content for global-scale terrestrial biosphere models. *Global Change Biology*, 15, 976–991.

Leblanc, S. G., Chen, J. M., White, H. P., Latifvic, R., Roujean, J. R., & Lacaze, R. (2005). Canada-wide foliage clumping index mapping from multi-angular POLDER measurements. *Canadian Journal of Remote Sensing*, 31, 364–376.

Leuning, R., Kelliher, F. M., de Pury, D. G. G., & Schulze, E. D. (1995). Leaf nitrogen, photosynthesis, conductance and transpiration: Scaling from leaves to canopy. *Plant, Cell & Environment*, 18, 1183–1200.

Liu, J., Chen, J. M., Cihlar, J., & Park, W. M. (1997). A process-based boreal ecosystem productivity simulator using remote sensing inputs. *Remote Sensing of Environment*, 62, 158–175.

Luo, H., Oechel, W. C., Hastings, S. J., Zulueta, R., Qian, Y., & Kwon, H. (2007). Mature semiarid chaparral ecosystems can be a significant sink for atmospheric carbon dioxide. *Global Change Biology*, 13, 386–396.

Ma, S. Y., Baldocchi, D. D., Xu, L. K., & Hehn, T. (2007). Inter-annual variability in carbon dioxide exchange of an oak/grass savanna and open grassland in California. *Agricultural and Forest Meteorology*, 147, 157–171.

Martin, T. A., & Jokela, E. J. (2004). Developmental patterns and nutrition impact radiation use efficiency components in southern pine stands. *Ecological Applications*, 14, 1839–1854.

Matsushita, B., & Tamura, M. (2002). Integrating remotely sensed data with an ecosystem model to estimate net primary productivity in East Asia. *Remote Sensing of Environment*, 81, 58–66.

Medlyn, B. E., Badek, F. -W., de Pury, D. G. G., Barton, C. V. M., Broadmeadow, M., Ceulemans, R., et al. (1999). Effects of elevated [CO2] on photosynthesis in European forest species: A meta-analysis of model parameters. *Plant, Cell & Environment*, 22, 1475–1495.

Monson, R. K., Sparks, J. P., Rosenstiel, T. N., Scott-Denton, L. E., Huxman, T. E., Harley, P. C., et al. (2005). Climatic influences on net ecosystem CO2 exchange during the transition from wintertime carbon source to springtime carbon sink in a high-elevation, subalpine forest. *Oecologia*, 146, 130–147.

Montieth, J. L. (1972). Solar radiation and production in tropical ecosystems. *Journal of Applied Ecology*, 9, 747–766.

Nightingale, J. M., Coops, N. C., Waring, R. H., & Hargrove, W. W. (2007). Comparison of MODIS gross primary production estimates for forests across the U.S.A. with those generated by a simple process model, 3-PGS. *Remote Sensing of Environment*, 109, 500–509.

Nilson, T. (1971). A theoretical analysis of the frequency of gaps in plant stands. *Agricultural Meteorology*, 8, 25–38.

Niu, S., Yuan, Z., Zhang, Y., Liu, W., Zhang, L., Huang, J., et al. (2005). Photosynthetic responses of C3 and C4 species to seasonal water variability and competition. *Journal of Experimental Botany*, 56, 2867–2876.

Noormets, A., McNulty, S. G., DeForest, J. L., Sun, G., Li, Q., & Chen, J. (2008). Drought during canopy development has lasting effect on annual carbon balance in a deciduous temperate forest. *New Phytologist*, 179, 818–828.

Noormets, A., McNulty, S. G., Gavazzi, M. J., Sun, G., Domec, J. C., King, J., et al. (2010). Response of carbon fluxes to drought in a coastal plain loblolly pine forest. *Global Change Biology*, 16, 272–287.

Norman, J. M. (1980). Interfacing leaf and canopy irradiance interception models. In J. D. Hesketh, & J. W. Jones (Eds.), *Predicting Photosynthesis for Ecosystem Models*, Vol. II. (pp. 49–67)Boca Raton, FL: CRC Press, Inc.

Norman, J. M. (1982). Simulation of microclimates. In J. L. Hatfield, & I. J. Thomason (Eds.), *Biometeorology in Integrated Pest Management* (pp. 65–99). New York: Academic Press.

Papale, D., & Valentini, R. (2003). A new assessment of European forests carbon exchanges by eddy fluxes and artificial neural network spatialization. *Global Change Biology*, 9, 525–535.

Paw, U. K. T., Falk, M., Suchanek, T. H., Ustin, S. L., Chen, J., Park, Y. -S., et al. (2004). Carbon dioxide exchange between an old-growth forest and the atmosphere. *Ecosystems*, 7, 513–524.

Pisek, J., & Chen, J. M. (2007). Comparison and validation of MODIS and VEGETATION global LAI products over four BigFoot sites in North America. *Remote Sensing of Environment*, 109, 81–94.

Pisek, J., Chen, J. M., Lacaze, R., Sonnentag, O., & Alikas, K. (2010). Expanding global mapping of foliage clumping index with multi-angular POLDER 3 measurements: evaluation and topographic compensation. *ISPRS Journal of Photgrammetry and Remote Sensing*, 65, 341–346.

Polcher, J., McAvaney, B., Viterbo, P., Gaertner, M. -A., Hahmann, A., Mahfouf, J. -F., et al. (1998). A proposal for a general interface between land-surface schemes and general circulation models. *Global and Planetary Change*, 19, 263–278.

Potter, C. S., Randerson, J. T., Field, C. B., Matson, P. A., Vitousek, P. M., Mooney, H. A., et al. (1993). Terrestrial ecosystem production: A process model based on global satellite and surface data. *Global Biogeochemical Cycles*, 7, 811–841.

Powell, T. L., Gholz, H. L., Clark, K. L., Starr, G., Cropper, W. P., & Martin, T. A. (2008). Carbon exchange of a mature, naturally regenerated pine forest in north Florida. *Global Change Biology*, 14, 2523–2538.

Prince, S. D., & Goward, S. N. (1995). Global primary production: A remote sensing approach. *Journal of Biogeography*, 22, 815–835.

Reichstein, M., Subke, J. A., Angeli, A. C., & Tenhunen, J. D. (2005). Does the temperature sensitivity of decomposition of soil organic matter depend upon water content, soil horizon, or incubation time? *Global Change Biology*, 11, 1754–1767.

Richardson, A. D., Anderson, R., Arain, M., et al. (2012). Terrestrial biosphere models need better representation of vegetation phenology: Results from the North American Carbon Program Site Synthesis. *Global Change Biology*, 18, 556–584.

Ruimy, A., Kergoat, L., Bondeau, A., et al. (1999). Comparing global models of terrestrial net primary productivity (NPP): Analysis of differences in light absorption and light-use efficiency. *Global Change Biology*, 5(S1), 56–64.

Sasai, T., Ichii, K., Nemani, R. R., & Yamaguchi, Y. (2005). Simulating terrestrial carbon fluxes using the new biosphere model "biosphere model integrating eco-physiological and mechanistic approaches using satellite data" (BEAMS). *Journal of Geophysical Research*, 110, G02014, http://dx.doi.org/10.1029/2005JG000045.

Scott, R. L., Hamerlynck, E. P., Jenerette, G. D., Moran, M. S., & Barron, G. (2010). Carbon dioxide exchange in a semidesert grassland through drought-induced vegetation change. *Journal of Geophysical Research*, 115, G03026.

Scott, R. L., Jenerette, G. D., Potts, D. L., & Huxman, T. E. (2009). Effects of seasonal drought on net carbon dioxide exchange from a woody-plant-encroached semiarid grassland. *Journal of Geophysical Research*, 114, G04004, http://dx.doi.org/10.1029/2008JG000900.

Sellers, P. J., Randall, D. A., Collatz, G. J., Berry, J. A., Field, C. B., Dazlich, D. A., et al. (1996). A revised land surface parameterization (SIB2) for atmospheric GCMs. Part I: Model formulation. *Journal of Climate*, 9, 676–705.

Sims, D. A., Rahman, A. F., Cordova, V. D., El-Masri, B. Z., Baldocchi, D. D., Bolstad, P. V., et al. (2008). A new model of gross primary productivity for North American ecosystems based solely on the enhanced vegetation index and land surface temperature from MODIS. *Remote Sensing of Environment*, 112, 1633–1646.

Sims, D. A., Rahman, A. F., Cordova, V. D., El-Masri, B. Z., Baldocchi, D. D., Flanagan, L. B., et al. (2006). On the use of MODIS EVI to assess gross primary productivity of North American ecosystems. *Journal of Geophysical Research*, 111, G04015, http://dx.doi.org/10.1029/2006JG000162.

Sprintsin, M., Chen, J. M., Desai, A. R., & Gough, C. (2012). Evaluation of leaf-to-canopy upscaling methodologies against carbon flux data in North America. *Journal of Geophysical Research*, 117, G01023, http://dx.doi.org/10.1029/2010JG001407.

Turner, D. P., Ritts, W. D., Cohen, W. B., Gower, S. T., Running, S. W., Zhao, M., et al. (2006). Evaluation of MODIS NPP and GPP products across multiple biomes. *Remote Sensing of Environment*, 102, 282–292, http://dx.doi.org/10.1016/j.rse.2006.02.017.

Turner, D. P., Ritts, W. D., Cohen, W. B., Gower, S. T., Zhao, M., Running, S. W., et al. (2003). Scaling gross primary production (GPP) over boreal and deciduous forest landscapes in support of MODIS GPP product validation. *Remote Sensing of Environment*, 88, 256–270.

Turner, D. P., Ritts, W. D., Cohen, W. B., Maeirsperger, T., Gower, S. T., Kirschbaum, A., et al. (2005). Site-level evaluation of satellite-based global terrestrial gross primary production and net primary production monitoring. *Global Change Biology*, 11, 666–684.

Urbanski, S., Barford, C., Wofsy, S., Kucharik, C., Pyle, E., Budney, J., et al. (2007). Factors controlling CO2 exchange on timescales from hourly to decadal at Harvard Forest. *Journal of Geophysical Research*, 112, G02020, http://dx.doi.org/10.1029/2006JG000293.

Van Wijk, M. T., Dekker, S. C., Bouten, W., Bosveld, F. C., Kohsiek, W., Kramer, K., et al. (2000). Modeling daily gas exchange of a Douglas-fir forest: Comparison of three stomatal conductance models with and without a soil water stress function. *Tree Physiology*, 20, 115–122.

Verma, S. B., Dobermann, A., & Cassman, K. G. (2005). Annual carbon dioxide exchange in irrigated and rainfed maize-based agroecosystems. *Agricultural and Forest Meteorology*, 131, 77–96.

Wang, S., Grant, R. F., Verseghy, D. L., & Black, T. A. (2001). Modelling plant carbon and nitrogen dynamics of a boreal aspen forest in CLASS-the Canadian Land Surface Scheme. *Ecological Modelling*, 142, 135–154.

Wang, Y. P., & Leuning, R. (1998). A two-leaf model for canopy conductance, photosynthesis and partitioning of available energy: I. Model description and comparison with a multi-layered model. *Agricultural and Forest Meteorology*, 91, 89–111.

Webb, R. S., Rosenzweig, C. E., & Levine, E. R. (1991). A global data set of soil particle size properties. *Tech. Memo.*, 4286, Greenbelt, Maryland, USA: NASA.

Wu, C., Chen, J. M., Desai, A. R., Hollinger, D. Y., Arain, M. A., Margolis, H. A., et al. (2012). Remote sensing of canopy light use efficiency in temperate and boreal forests of North America using MODIS imagery. *Remote Sensing of Environment*, 118, 60–72.

Wu, C., Munger, J. W., Niu, Z., & Kuang, D. (2010). Comparison of multiple models for estimating gross primary production using MODIS and eddy covariance data in Harvard Forest. *Remote Sensing of Environment*, 114, 2925–2939.

Wullschleger, S. D. (1993). Biochemical limitations to carbon assimilation in C3 plants —A retrospective analysis of the A/Ci curves from 109 species. *Journal of Experimental Botany*, 44, 907–920.

Xiao, J., Zhuang, Q., Law, B., Chen, J., Baldocchi, D., Cook, D., et al. (2010). A continuous measure of gross primary production for the conterminous United States derived from MODIS and AmeriFlux data. *Remote Sensing of Environment*, 114, 576–591.

Yang, F., Ichii, K., White, M. A., Hashimoto, G., Michaelis, A. R., Votava, P., et al. (2007). Developing a continental-scale measure of gross primary production by combining MODIS and AmeriFlux data through Support Vector machine approach. *Remote Sensing of Environment*, 110, 109–122.

Zhang, F. M., Ju, W., Chen, J. M., Wang, S., Yu, G., Zhao, X., et al. (2010). Preliminary study on evapotranspiration in East Asia using the BEPS ecological model. *Journal of Natural Resources*, 25(9), 1596–1606.

Zhao, M., Heinsch, F. A., Nemani, R. R., & Running, S. W. (2005). Improvements of the MODIS terrestrial gross and net primary production global data set. *Remote Sensing of Environment*, 95, 164–176.

Zhao, M. S., & Running, S. W. (2010). Drought-induced reduction in global terrestrial net primary production from 2000 through 2009. *Science*, 329, 940–943, http://dx.doi.org/10.1126/science.1192666.

Zhao, M., Running, S. W., & Nemani, R. R. (2006). Sensitivity of moderate resolution imaging spectroradiometer (MODIS) terrestrial primary production to the accuracy of meteorological reanalyses. *Journal of Geophysical Research*, 111(G01002), http://dx.doi.org/10.1029/2004JG000004.6.

Zierl, B. (2001). A water balance model to simulate drought in forested ecosystems and its application to the entire forested area in Switzerland. *Journal of Hydrology*, 242, 115–136.